Web: www.witpress.com Email witpress@witpress.com
Paper from: *Advanced Computational Methods in Heat Transfer*, B Sunden and CA Brebbia (Editors).
ISBN 1-85312-906-2

Numerical simulation of induction heating processes; comparison between direct multi-harmonic and classical staggered approaches

R. Pascal[1,2], P. Conraux[2] & J.M. Bergheau[1]
[1]*LTDS, UMR5513 CNRS/ECL/ENISE,*
58 rue J.Parot, 42023 Saint Etienne Cedex 2, France
[2]*ESI SOFTWARE,*
84 Bvd Vivier Merle, 69485 LYON Cedex 03 , France

Abstract

Numerical simulation of induction heating processes rests on the modelling of coupled thermal and magnetodynamic analyses. Strong couplings come from, on one hand, the power dissipated through Joule effect due to eddy currents, and on the other hand, electromagnetic properties that depend on temperature. Different methods can be used to perform such simulations. The aim of this paper is to compare a new fully coupled direct method where both phenomena are solved together with a more classical staggered approach.

1 Introduction

Any electrical conductor placed in a time-varying magnetic field is the seat of eddy currents that dissipate power through Joule effect. This power is concentrated at the surface of the component, in a small thickness which depends on the electric conductivity and magnetic permeability of the material, but also on the frequency of the current. Induction hardening processes for example, take advantage of this effect because it is therefore possible to control the thickness of the treated layer.

The simulation of induction heating processes rests on the solution of coupled magnetodynamic and thermal problems and comes up against several difficulties. A first difficulty comes from the fact that electromagnetic and thermal phenomena

Paper from: *Advanced Computational Methods in Heat Transfer*, B Sunden and CA Brebbia (Editors).
ISBN 1-85312-906-2

time constants differ considerably. Indeed, the working frequency usually encountered with induction hardening applications, for example, are of the order of magnitude of a few tens of kHz. As compared to those frequencies, thermal phenomena vary very slowly. A second difficulty comes from the very strong non-linearities of the problem: non-linear magnetization curves, thermal non-linearities, temperature dependent on the electromagnetic properties specifically near the Curie temperature.

For obvious computation time-related reasons, it is unreasonable to perform a fully coupled magnetodynamic and thermal analysis using time steps corresponding to magnetodynamics, which would be of the order of $10^{-7}s$. Such analysis would require several million of time steps. Moreover, temperature variations within each time step would be unsignificant leading therefore to large computation errors.

The staggered approach is based on successive magnetodynamic and thermal resolutions with an update of data issued from one and intended for the other one until the accuracy required on temperature is reached, ref [1]. Magnetodynamic analyses are performed using their own time steps and the Joule power taken into account in the heat equation is the mean Joule power over one source current period. This method needs large computation times even for 2D or axisymmetrical studies.

The alternative we propose is to solve both problems simultaneously using a new finite element formulation, ref [2]. This formulation rests on a multi-harmonic decomposition of the magnetic vector potential, ref [3][4][5]. The mean power corresponding to one period of currents is calculated and directly taken into account in the heat equation.

Both approaches have been implemented in the finite element code SYSWELD®, ref [6]. They are first presented in sections 2 and 3 and then compared in section 4. The results and the efficiency of the new approach will be discussed.

2 Staggered method

The aim of this part is to briefly present the basis of the classical staggered method for the modelling of magneto-thermal couplings, ref [1].

At each thermal time step, see figure 1, a magnetodynamic analysis is performed for 5 or 6 periods of the source current in order to reach the periodic state. Time integration is achieved using an implicit finite difference scheme to take accurately into account the magnetic non-linearity coming from the magnetization curve. The time step Δt_{mag} used for the magnetodynamic analysis is equal to one hundredth of the current period. The results of this calculation are the current density and the heat generated through Joule effect at each magnetodynamic time step. The power dissipation is then averaged over a source current period. This value is then taken into account in the thermal analysis for the computation of the new temperature field.

Paper from: *Advanced Computational Methods in Heat Transfer*, B Sunden and CA Brebbia (Editors).
ISBN 1-85312-906-2

Different coupling levels can be considered. The first one consists in updating the power dissipation at the beginning of each thermal time step (time $t + \Delta t_{ther}$) using the temperature computed at the previous thermal time step (time t) and to use it for the computation of temperature at time $t + \Delta t_{ther}$ and so on. The second coupling level is the strongest one. In this case, after calculating the new temperature distribution, an additional loop-back to the magnetodynamic analysis is achieved in order to ensure that both magnetodynamic and thermal problems are accurately solved at the same time.

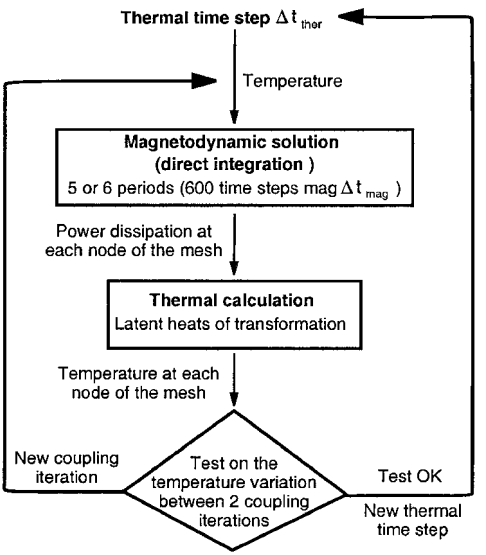

Figure 1: Staggered method

3 Direct method

As introduced before, the aim of this method is to strongly couple both electromagnetic and thermal fields in the same finite element.

Insofar as sinusoidal source currents are considered, the Harmonic Balance Finite Element Method, ref [3][4], can be used. This method consists in calculating the first terms of the Fourier series of the solution instead of performing a transient analysis. Indeed, in the case of a purely sinusoidal excitation, when the problem is linear, the solution is purely sinusoidal too. When non-linear magnetization curves have to be considered, as it is the case for steels, then the solution contains other impair harmonics. The electromagnetic quantities can therefore be expressed

Paper from: *Advanced Computational Methods in Heat Transfer*, B Sunden and CA Brebbia (Editors).
ISBN 1-85312-906-2

through Fourier series as follows:

$$\mathbf{X}(\vec{x},t) = \sum_{k=1,3,\ldots}^{m} \left(\mathbf{X}_{kc}(\vec{x}) \cos(k\omega t) + \mathbf{X}_{ks}(\vec{x}) \sin(k\omega t) \right) \tag{1}$$

where ω is the fundamental angular frequency that is the angular frequency of the source currents.

From Maxwell's equations, neglecting displacement currents and introducing the magnetic vector potential $\mathbf{A}$, the magnetodynamic problem can be written as follows:

$$\sigma \frac{\partial \mathbf{A}(\vec{x},t)}{\partial t} + \mathbf{rot}\,(\nu\,.\,\mathbf{rot}\,\mathbf{A}(\vec{x},t)) - \mathbf{J_0}(\vec{x},t) = 0 \tag{2}$$

$$\text{with} \quad \operatorname{div} \mathbf{A}(\vec{x},t) = 0 \tag{3}$$

where σ is the electric conductivity, ν, the magnetic reluctivity ($\nu = \frac{1}{\mu}$, μ being the magnetic permeability) and $\mathbf{J_0}$, the source current density. Equations 2 and 3 are valid in the whole space. When bounded domains are considered, boundary conditions have to be added.

In the case of an axisymmetrical geometry around an axis $\mathbf{e}_z$ and for circonferential source currents only depending on radial and axial coordinates (r,z):

$$\begin{aligned} \mathbf{J_0}(\vec{x},t) &= J_0(r,z,t)\,\mathbf{e}_\theta \\ &= \sum_{k=1,3}^{m} \left(J_{0kc}(r,z)\cos(k\omega t) + J_{0ks}(r,z)\sin(k\omega t) \right)\,\mathbf{e}_\theta \end{aligned} \tag{4}$$

then, the problem is axisymmetric and the magnetic vector potential only presents one non-zero component $A(r,z,t)$:

$$\begin{aligned} \mathbf{A}(\vec{x},t) &= A(r,z,t)\,\mathbf{e}_\theta \\ &= \sum_{k=1,3}^{m} \left(A_{kc}(r,z)\cos(k\omega t) + A_{ks}(r,z)\sin(k\omega t) \right)\,\mathbf{e}_\theta \end{aligned} \tag{5}$$

Considering equation (5), one can note that equation (3) is automatically satisfied and that equation (2) only has to be solved in direction $\mathbf{e}_\theta$.

Because only the terms $l = 1,3,\ldots,m$ of the Fourier series of the magnetic vector potential have to be calculated, equation (2) is now replaced by the following equations, ref [2], with $l = 1,3,\ldots,m$:

$$\frac{2}{T}\int_0^T \left(\sigma \frac{\partial \mathbf{A}}{\partial t} + \mathbf{rot}\,(\nu\,.\,\mathbf{rot}\,\mathbf{A}) - \mathbf{J_0} \right).\cos(l\omega t)\,dt = 0 \tag{6}$$

$$\frac{2}{T}\int_0^T \left(\sigma \frac{\partial \mathbf{A}}{\partial t} + \mathbf{rot}\,(\nu\,.\,\mathbf{rot}\,\mathbf{A}) - \mathbf{J_0} \right).\sin(l\omega t)\,dt = 0 \tag{7}$$

Paper from: *Advanced Computational Methods in Heat Transfer*, B Sunden and CA Brebbia (Editors).
ISBN 1-85312-906-2

Obviously, the accuracy of the solution depends on the number of harmonics taken into account. Nevertheless, the gain in accuracy is counterbalanced by an increase of the problem size.

For the thermal analysis, the following equations have to be solved:

$$\rho C \frac{d\theta}{dt} - \mathrm{div}(\lambda . \mathbf{grad}\,\theta) - Q = 0 \quad \text{in } \Omega \tag{8}$$

$$\lambda . \mathbf{grad}\,\theta . n = q(\theta, t) \qquad \text{on } \partial\Omega_\theta \tag{9}$$

$$\theta = \theta_p(t) \qquad \text{on } \partial\Omega_\theta \qquad \text{with } \partial\Omega = \partial\Omega_q \cup \partial\Omega_\theta \tag{10}$$

In the above equations, θ represents temperature and $\rho(\theta)$, $C(\theta)$, $\lambda(\theta)$ are the density, the specific heat and the thermal conductivity respectively. Ω is a bounded domain representing all the conductive media.
Q represents the power losses through Joule effect. The mean power over one period T of the source current is considered:

$$Q(\vec{x}) = \frac{1}{T} \int_0^T \mathbf{J}(\vec{x}, t) . \mathbf{E}(\vec{x}, t) \tag{11}$$

where $\mathbf{J}$ and $\mathbf{E}$ are the electric field and the current density respectively.
Considering the Fourier series decomposition of the magnetic vector potential, Q can be written as follows:

$$Q(\vec{x}) = \frac{1}{2}\, \sigma(\theta)\, \omega^2 . \sum_{k=1,3}^{m} k^2 \left((\mathbf{A}_{kc}(\vec{x}))^2 + (\mathbf{A}_{ks}(\vec{x}))^2 \right) \tag{12}$$

The finite element approximation uses $m+2$ degrees of freedom at each node (m being the order of the highest harmonic considered), namely the temperature and the sine and cosine parts of the $\frac{m+1}{2}$ harmonics of the magnetic vector potential. The scheme of this method is presented in figure 2.
The application of the finite element method then leads to the resolution of a system of $m+2$ coupled non-linear equations for each node and at each thermal time step:

$$\left\{ \begin{array}{c} \{\mathbf{R}_1(\{\theta\}, \{A_{1c}\}, \{A_{1s}\}, \ldots)\} = 0 \\ \{\mathbf{R}_2(\{\theta\}, \{A_{1c}\}, \{A_{1s}\}, \ldots)\} = 0 \\ \{\mathbf{R}_3(\{\theta\}, \{A_{1c}\}, \{A_{1s}\}, \ldots)\} = 0 \\ \ldots \end{array} \right\} \tag{13}$$

The first equation in (13) corresponds to the thermal problem. The $m+1$ other equations correspond to the finite element formulation associated with equations 6 and 7. These equations are solved using the Newton-Raphson method. Iterations are performed untill either the maximum absolute value of the nodal residual (equation 13) or the maximum variation of degrees of freedom between two

Paper from: *Advanced Computational Methods in Heat Transfer*, B Sunden and CA Brebbia (Editors).
ISBN 1-85312-906-2

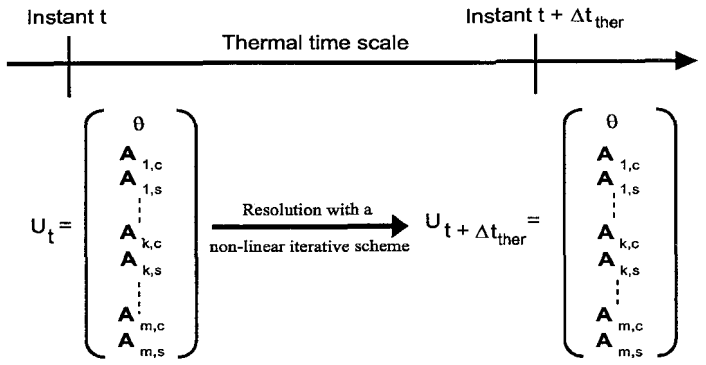

Figure 2: Direct method

successive iterations become less than prescribed thresholds. In our case, these thresholds are defined proportionaly to the values obtained at the beginning of the iteration process using coefficient $\epsilon = 10^{-3}$.

4 Application

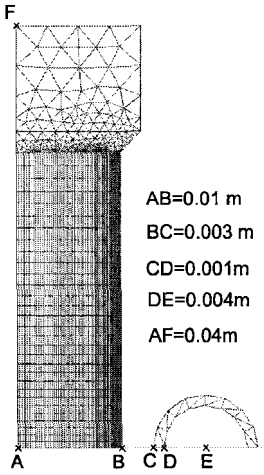

Figure 3: Mesh of the device - steel part and inductor

In order to compare both methods, we consider the heating of a steel piece using a static single turn copper inductor. The simulation is performed under an

Paper from: *Advanced Computational Methods in Heat Transfer*, B Sunden and CA Brebbia (Editors).
ISBN 1-85312-906-2

axisymmetric assumption and for symmetry reasons, only half of a meridian section is considered (figure 3). One can note that magnetodynamic analysis requires meshing of the air that has not been represented in figure 3. The finite element mesh is progressively refined from the center to the surface of the component and adapted to the parameters of the problem. In fact, the number of elements have to be increased near the surface of the component where eddy currents are the most important (skin effect). The whole mesh includes 3705 elements and 3132 nodes.

The electromagnetic properties of the component are temperature dependent. The magnetization curves and the electric conductivity are given in figures 4 and 5 respectively. The following thermal properties have been considered: $\rho = 7800\, kg.m^{-3}$, $C = 460\, J.kg^{-1}.K^{-1}$ and $\lambda = 30\, W.m^{-1}.K^{-1}$. A sinusoidal voltage $V_{1c} = 4.5\, Volts$ and the frequency of which is equal to $50\, kHz$ is applied to the inductor during $2,6\, s$. These operating conditions could correspond to induction hardening applications.

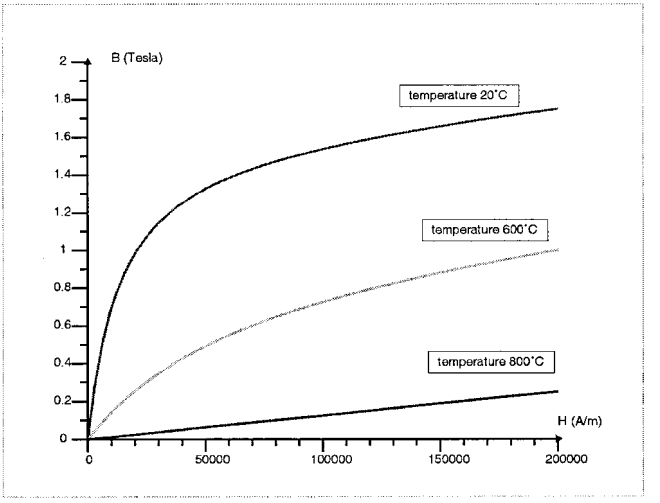

Figure 4: Magnetization curves as a function of temperature

Three simulations have been performed using the finite element software SYSWELD®. Simulation 1 corresponds to the staggered approach. Simulation 2 uses the direct approach presented previously with only one harmonic whereas simulation 3 uses harmonics 1 and 3. A thermal time step $\Delta t_{ther} = 0,025\, s$ has been chosen for all the simulations. In the same way, the accuracy associated with Newton-Raphson solution procedure is the same for all the simulations. Figure 6 summarizes the characteristics of all the simulations that have been performed.

At the begining of heating, the skin depth is about 0,3 mm whereas it is about 2,7 mm at the end. This comes from the fact that the magnetization curve is temperature dependent. At the beginning of heating, the material is cold and so, the magnetic permeability is high leading to small skin depths. At the end of heating,

Paper from: *Advanced Computational Methods in Heat Transfer*, B Sunden and CA Brebbia (Editors).
ISBN 1-85312-906-2

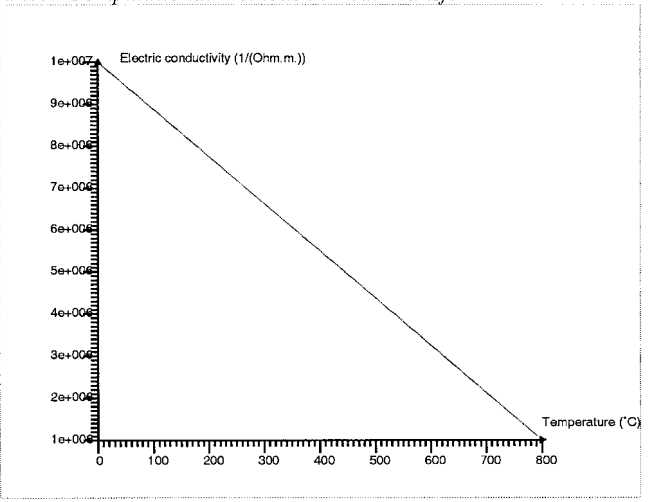

Figure 5: Electric conductivity as a function of temperature

a large part of the material has exceeded the Curie temperature leading therefore to large skin depths. For simulation 1, all transient magnetodynamic analyses have been performed over 6 periods of the source currents ($T = 2 * 10^{-5}\ s$) with time step equal to one hundredth of the period ($\Delta t_{mag} = 0.01 * T$). The main part of the computation effort comes from the magnetodynamic calculation sequences which are necessary at each thermal time step. At least, 2 strong coupling loops have been necessary to obtain a good convergence of the temperature (convergence is supposed to be reached when the temperature change between 2 successive iterations is less than 2°C).

	1) Staggered method	2) Direct method 1st order harmonic	3) Direct method 1st and 3rd order harmonics
Number of temperature cards	104	104	104
Thermal time step	0.025s	0.025s	0.025s
Maximum error on temperature in comparison with simulation 1		1 %	1 %
CPU computation time Elapsed time	CPU = 116 515 49H	CPU = 23 642 6h40	CPU = 112093 31h45
Total number of magnetodynamic analysis sequences	233		
Same computer for all simulations: PC PentiumIII 1Ghz RAM=512MO			

Figure 6: Characteristics of the different simulations

Paper from: *Advanced Computational Methods in Heat Transfer*, B Sunden and CA Brebbia (Editors).
ISBN 1-85312-906-2

Figure 7 gives temperature profiles between points A and B (see figure 3) at different times from 0,1 s to 2,6 s every 0,1 s and corresponding to simulation 2. At the end of process simulation, the temperature has reached a maximum of about 1130°C at the surface in A and 380°C in B. If now these profiles are subtracted from those calculated with simulation 1, we obtain the curves given in figure 8.

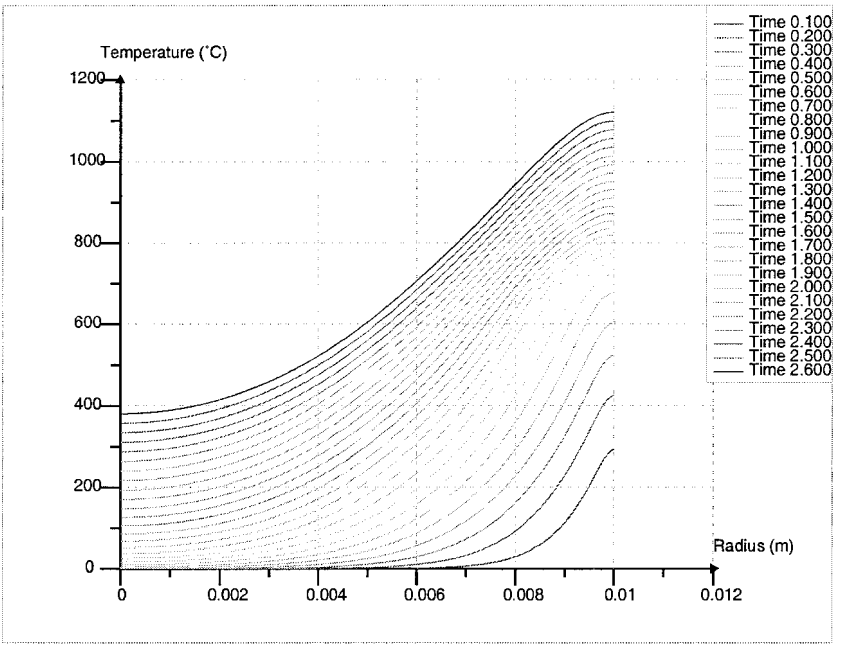

Figure 7: Temperature profiles between points A and B of figure 3 every 0.1s - Direct approach

Figure 8 then shows that the maximum temperature difference between staggered and direct (1 harmonic) simulations is less than 1% whereas the total elapsed time is approximatively reduced by a factor 7 with simulation 2. After comparing the results of simulations 2 and 3, one can deduce that the introduction of the third harmonic of the magnetic vector potential has no significant influence on the temperature field whereas the CPU time is largely increased. In fact, the magnitude of the fundamental harmonic (sine and cosine parts) is approximately 200 times bigger than the one of the third order harmonic. This ratio, reported in equation (12), confirms that the contribution of the third order harmonic can be obviously neglected in the calculation of the power losses. This large ratio between magnitudes of harmonics 1 and 3 can be explained by the fact that, in our case and for all heating problems where the magnetic field magnitude is very high, the material is magnetically oversatured. So the most important part of the magnetization curve is the one corresponding to $H > 10^5 Am^{-1}$. In other words, material reacts as if its magnetic permeability was constant. On the other hand, the more the temperature

Paper from: *Advanced Computational Methods in Heat Transfer*, B Sunden and CA Brebbia (Editors).
ISBN 1-85312-906-2

increases, the more the magnetization curve is linear. For applications involving smaller levels of saturation, there is no doubt that the direct approach using several harmonics will give more accurate results.

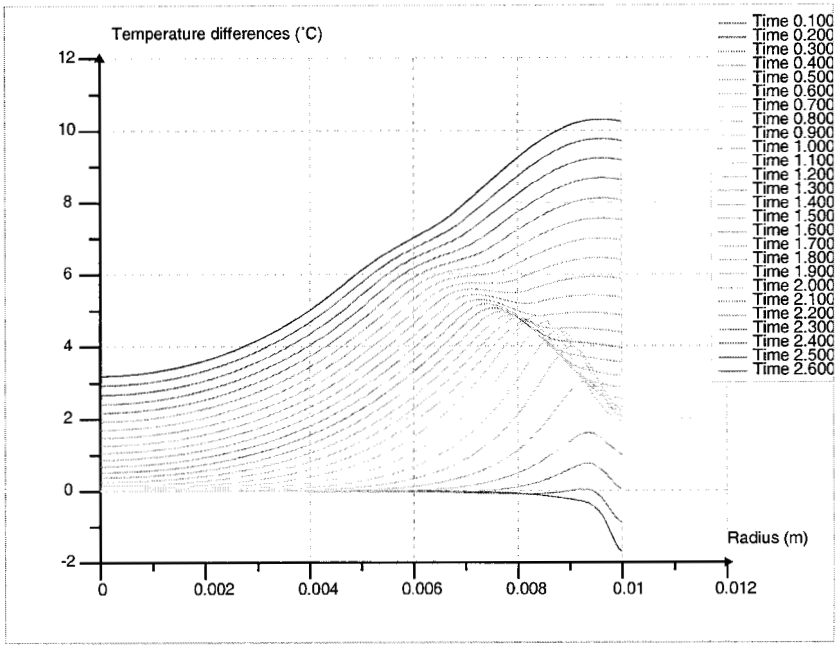

Figure 8: Temperature differences between direct (1 harmonic) and staggered methods between points A and B every 0.1s

One could think that the staggered approach gives the most accurate results as magnetic non linearities are precisely taken into account. Nevertheless, one drawback of the transient magnetodynamic analysis is that the solution must be stabilized. Therefore, calculations must cover several periods of the source current. In fact, one can observe that even after reaching some solution which seems to be stabilized, a very slow decrease of the magnetic vector potential magnitude is still going on. For simulation 1, we chose 6 periods that seems to be a good compromise between time consumption and accuracy of the electromagnetic fields. Moreover, a precision equal to 2°C on the temperature variation between 2 successive iterations has been considered for the coupling between magnetodynamic and thermal analyses. With the direct method, the calculation precision at each thermal time step is the one of the Newton-Raphson procedure which is very much smaller than 2°C. We can therefore conclude that both approaches give the same level of accuracy.

Another advantage of the direct method comes from the fact that both phenomena are solved together in the same finite element. For the staggered method, successive magnetodynamic and thermal analyses are performed with a lot of sav-

Paper from: *Advanced Computational Methods in Heat Transfer*, B Sunden and CA Brebbia (Editors).
ISBN 1-85312-906-2

ings and readings on the physical disk of the computer. The gain in time in choosing the direct approach instead of the staggered one can therefore be important as it can be seen in figure 6.

5 Conclusion

We have presented two approaches for the simulation of induction heating processes. Both methods have been compared on a simple induction hardening example. It has been shown that the direct method gives promising results as it leads to the same level of accuracy as the staggered method but for computation times 7 times smaller. The direct method enables to consider several harmonics of the magnetic vector potential. However, simulations using, on one hand, the fundamental harmonic only and, on the other hand, harmonics 1 and 3 have not pointed out any significant difference on the simple example that has been considered. This probably comes from the operating conditions that have been chosen for this example.

References

[1] Bergheau, J-M. & Conraux, Ph. FEM-BEM Coupling for the Modelling of Induction Heating Processes Including Moving Parts. *Proc. of the 1st International Conference on Thermal Process Modelling and Computer Simulation,* Journal of Shangai Jiaotong University, ed H. Zheng, Shangai, Vol E-5 no 1 pp.91-99, June 2000.

[2] Pascal, R., Bergheau, J-M. & Conraux, Ph. Direct coupling between magnetodynamic and thermal analysis allowed by a multi-harmonic decomposition of magnetic vector potential. *Proc. of the 13th COMPUMAG,* ed A. Nicolas, Evian, Vol 3 pp.94-95, July 2-5 2001.

[3] Yamada, S., Bessho, K. & Lu, J. Harmonic balance finite element method applied to nonlinear ac magnetic analysis. *IEEE Transactions On Magnetics,* Vol 25 no 4 pp.2971-2973, July 1989.

[4] Lu, J., Yamada, S. & Bessho, K. Time-Periodic magnetic field analysis with saturation and hysterisis characteristics by harmonic balance finite element method. *IEEE Transactions On Magnetics,* Vol 26 no 2 pp.995-998, March 1990.

[5] Gyselinck, J., Dular P., Geuzaine, C. & Legros, W. Harmonic balance finite element modelling of electromagnetic devices: a novel approach. *IEEE Transactions On Magnetics,* to be published.

[6] SYSTUS®2000, SYSWELD®2000, SYSMAGNA™2000, User's manual, ESI Software, 2000.